

EFFECT OF ALKALI METAL OXIDES ON THE SURFACE ENERGY OF CERAMIC GLAZE

HONGQUAN ZHANG*, WENJING ZHAO*, #JIN WEN*, YE LI**

*School of Materials Science and Engineering, Wuhan University of Technology, Wuhan 430070, PR China

**School of Resources and Environmental Engineering, Wuhan University of Technology, Wuhan 430070, PR China

#E-mail: wen9888@Hotmail.com

Submitted February 23, 2023; accepted March 28, 2023

Keywords: Ceramic glaze, Glossiness, Network structure, Surface energy, Water wettability, Antifouling and easy cleaning

A transparent ceramic glaze with good apparent quality and water wettability was successfully prepared by adjusting the mass fraction ratio of $\text{Na}_2\text{O}/\text{K}_2\text{O}$ and $\text{R}_2\text{O}/\text{Al}_2\text{O}_3$ at 1280 °C. The effects of the $\text{Na}_2\text{O}/\text{K}_2\text{O}$ and $\text{R}_2\text{O}/\text{Al}_2\text{O}_3$ ratios on the surface energy and glossiness of the ceramic glaze were studied in the present work. The results show that the mass fraction ratio of $\text{Na}_2\text{O}/\text{K}_2\text{O}$ and $\text{R}_2\text{O}/\text{Al}_2\text{O}_3$ showed an obvious effect on the high temperature viscosity and melting temperature of the glaze, the density of the glaze network structure and the number of broken bonds on the glaze. When $\text{Na}_2\text{O}/\text{K}_2\text{O} = 0.8 - 1.6$, $\text{R}_2\text{O}/\text{Al}_2\text{O}_3 = 0.8 - 1.2$, the glaze showed a glossiness of 88.3 – 108.3 with a 0.11 – 12 % increase, and the surface energy of 70.17 – 78.5 $\text{mJ}\cdot\text{m}^{-2}$ with a 5.62 – 29.55 % increase, being obviously higher than those of the basic glaze. The greater the surface energy of the glaze was, the greater the polarity component was, and the better the wettability of the water on the glaze was, which would be conducive to improving the antifouling and easy cleaning of ceramic products.

INTRODUCTION

Ceramic products are widely used in architecture, interior and exterior decorations, kitchen and sanitary wares, and the daily life of families. However, ceramic glazes are frequently contaminated by dust, dirt, or kitchen oil during use, which not only requires a lot of manpower to clean, but also easily cause potential threats to one's health if too many detergents are used. Thus, in recent years, attention has been drawn to how easily the ceramic product can be cleaned and that they are anti-fouling [1].

To improve the anti-pollution and self-cleaning performance of materials, up to now, two surface anti-fouling technical approaches are often used: surface coating treatments and adjusting the surface composition. Surface coating treatments are one kind of commonly used technology, which usually include super hydrophobic technologies and super hydrophilic technologies. A super-hydrophobic surface usually requires the material to have a slip angle to be less than 10 degrees and a contact angle to be higher than 150 degrees. In order to obtain a material surface to be super-hydrophobic [2], super-hydrophobic surface treatments are made on the material surface with organic solutions [3, 4], or adopting a micronanometre super-hydrophobic surface design method so as to obtain surfaces with a larger water contact angle and smaller sliding angle [5, 6], which assist in keeping droplets to be spherical in shape to make them simple enough to glide over the material surface and remove

any polluting particles. For extremely hydrophilic surfaces, the surface has a water contact angle of less than 5° and a droplet diffusion time of less than 0.5 s [7]. Such a technology is usually required to generate a hydrophilic coating on the material surface through the photo-induced super hydrophilicity of TiO_2 [8, 9]. The substantially strong affinity for water could result in a lower surface area between the dust particles and the coating and a lower capacity for electrostatic adsorption. Moreover, water droplets may pass through the coating-dust contact, causing the dust or dirt to be simply washed away by the water flow. Nonetheless, whether a surface is super-hydrophobic or super hydrophilic, the technical specifications of producing them are very stringent, and the product's shelf life is very short due to the poor wear and tear characteristics during usage as well as the high production costs, which make industrial batch manufacturing inappropriate.

Another antifouling technology, i.e., adjusting the surface composition technology, includes an antibacterial ceramic glaze technology and an intelligent cleaning glaze technology. The antibacterial ceramic glaze technology involves adding antibacterial agents to the ceramic glaze, such as photocatalytic antibacterial agents [10] or antibacterial metal ions, such as Ag, Cu, Zn, etc. [11-13]. Although this technology could make the ceramic surfaces more resistant to bacteria and viruses and depress their survival rate on the ceramic surface, it cannot actually make the ceramic surfaces easier to clean. The intelligent and clean glaze technology

applies a layer of metal ions on the glaze that reacts with the soiling substances on the ceramic surface to decrease the adherence of dirt and prevents the generation of black spots. Nevertheless, the massive alkali metal ions in the ceramic glaze make the melting temperature of the glaze to often be low, leading to the glaze having a medium hardness, strength, and wear resistance [14].

The ceramics themselves have water wettability, and their anti-fouling and easy cleaning ability have been found to be closely related to the surface energy of the glaze and its contact angle with the liquid on the surface [1]. The better the hydrophilicity of the glaze, the easier it is for the water to spread into a water film on the glaze, which helps to block the contact between the dirt and the glaze, so that the dirt can be easily carried away by the flow of water. The chemical composition and surface structure of ceramic glazes have an impact on their wettability [15], although the relationship between the surface structure and water wettability of ceramic products have extensively been studied in the past decades, little research has been undertaken on the effect of the glaze composition on the surface energy and water wettability of the glaze. Thus, this study combines the above two methods and mainly refers to the cleaning principle of superhydrophilic technologies [16-18] to adjust the chemical composition of the glaze, as well as to especially focus on the impacts of alkali metal oxides and their ratio to Al_2O_3 on the surface energy and polarity components, to improve the wettability of water on the glaze and obtain a ceramic glaze with improved an anti-fouling and easier cleaning performance.

EXPERIMENTAL

Experimental design and process

The composition of the glaze commonly used for domestic ceramics was selected as the basic ingredient, and the experimental glaze composition was designed using a method of controlling the single factor variables. The contents of Na_2O and K_2O changed from 0 to 10 % based on the selected basic glaze ingredient, the mass proportion of the other remaining oxides being relatively unchanged, in which the mass ratio of $\text{Na}_2\text{O}/\text{K}_2\text{O}$ were changed from 0.8 to 2 and that of alkali metal oxide $\text{R}_2\text{O}/\text{Al}_2\text{O}_3$ in the glaze from 0.8 to 1.2. The glaze pastes composed by Na_2CO_3 , K_2CO_3 , MgO , CaO , potash feldspar, kaolin and a quartz mixture were prepared by wet ball milling for 1 h. After the ceramic green bodies were prepared using traditional ceramic paste by pressing in a mould, the mouldings were dried. The glaze pastes were applied on the final samples by a dipping method. Finally, the ceramic materials were fired at 1280 °C for 30 min, and then cooled naturally with a furnace.

Performance characterisation

To ensure the glaze quality, preliminary screening was carried out by observing whether there were obvious defects in the glaze and whether the glossiness and surface energy of the glaze were larger than or equal to that of the basic sample. The contact angle of the ceramic glaze surfaces was measured by a contact angle meter (SL200A, USA). The solid surface energy and its dispersion component and polarity component of the glaze surface were calculated by measuring the contact angle of two liquids with a known surface tension on the solid surface according to Young's equation using the Owens, Wendt, Rabel and Kaelble (WORK) method, i.e., the geometric average method [19], in which distilled water and ethylene glycol were selected as the test liquids in the present experiment. The glossiness of the samples was measured by a gloss meter (WGG-60, China). The surface morphology was observed by a scanning electron microscope (Quant 450FEG, FEI, USA). The silicon coordination in the glaze layer was characterised by a solid-state nuclear magnetic resonance spectrometer (NMR) (Advance III 400MHz, Bruker).

RESULTS AND DISCUSSION

Changes in the glaze glossiness

The chemical composition and properties of the basic glaze are listed in Table 1. The glossiness of the basic glaze sample was 83.6 and the surface energy was $70.09 \text{ mJ}\cdot\text{m}^{-2}$, which could effectively meet the commercial requirements of daily ceramic products. Based on the basic glaze composition and maintaining a $\text{Na}_2\text{O}/\text{K}_2\text{O}$ ratio of 0.67 – 2.0 and a $\text{R}_2\text{O}/\text{Al}_2\text{O}_3$ ratio of 0.72 – 1.26, the previous single factor study on the effects of alkali metal oxides on the surface energy and glossiness of the ceramic glaze found that the contents of Na_2O and K_2O as well as the ratio of the alkali metal oxides ($\text{R}_2\text{O}: \text{Na}_2\text{O} + \text{K}_2\text{O}$) to the Al_2O_3 content ($\text{R}_2\text{O}/\text{Al}_2\text{O}_3$) showed an obvious effect on both the surface energy and glossiness, giving a glaze glossiness of 88.3 – 112.6 and a surface energy of $70.62 - 78.62 \text{ mJ}\cdot\text{m}^{-2}$. Thus, on the premise of ensuring the glossiness being higher than or equal to the basic sample, the $\text{Na}_2\text{O}/\text{K}_2\text{O}$ ratio was varied at 0.8, 1.2, 1.6, 1.8 and 2, and the $\text{R}_2\text{O}/\text{Al}_2\text{O}_3$ changed at 0.8, 0.9, 1.0, 1.1 and 1.2, in the present study.

Figure 1 shows changes in the glossiness (GU) with $\text{Na}_2\text{O}/\text{K}_2\text{O}$ under the different $\text{R}_2\text{O}/\text{Al}_2\text{O}_3$ ratios. The glossiness first increased and then decreased with an increase in $\text{Na}_2\text{O}/\text{K}_2\text{O}$. When $\text{Na}_2\text{O}/\text{K}_2\text{O} = 0.8 - 1.6$ and $\text{R}_2\text{O}/\text{Al}_2\text{O}_3 = 0.8 - 1.2$, the glossiness of the obtained sample varied between 88.3 – 108.3, being larger than that of the basic sample (Table 1). Whereas, when $\text{Na}_2\text{O}/\text{K}_2\text{O}$ was greater than 1.6, the glossiness began to obviously decrease, giving a lower value of 80.9

Table 1. Chemical composition and properties of the basic glaze.

Chemical composition (wt. %)						Glaze properties		
SiO ₂	Al ₂ O ₃	CaO	MgO	Na ₂ O	K ₂ O	γ_s (mJ·m ⁻²)	γ_s^d (%)	Gloss
59.00	11.12	14.16	2.02	6.12	7.58	70.09	93.43	83.6

when compared with that of the basic sample at $\text{Na}_2\text{O}/\text{K}_2\text{O} = 2$ and $\text{R}_2\text{O}/\text{Al}_2\text{O}_3 = 1.1$. It can be seen from the above results that the glossiness of the glaze could be improved by properly increasing the relative content of Na_2O at $\text{R}_2\text{O}/\text{Al}_2\text{O}_3 = 0.8 - 1.2$.

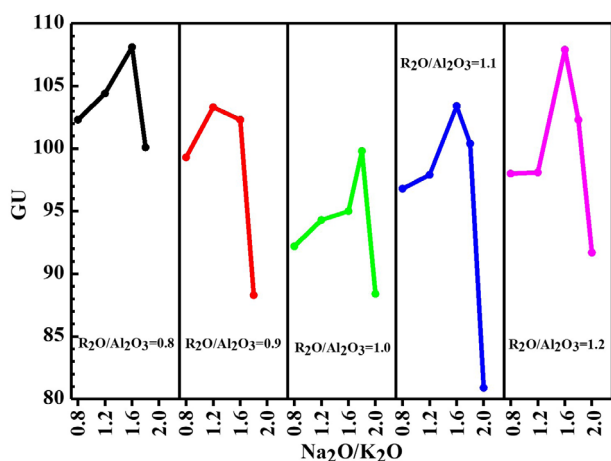


Figure 1. Variation trend of the ceramic glaze glossiness (GU) with $\text{Na}_2\text{O}/\text{K}_2\text{O}$.

In general, the glossiness of a ceramic glaze is related to the refractive index of the glaze and depends on the specular reflection degree of light on the glaze. To a certain extent, it also reflects the smoothness degree of the glaze surface, that is, the fewer defects in the glaze, the smoother the glaze, the stronger the reflection effect, and the higher the glossiness [20]. Na_2O and K_2O , as network modifiers in the network structure of silicate glass, can provide “free oxygen” to break the Si–O network and reduce the glaze melting temperature. In addition, the alkali metal ion R^+ has a reverse polarisation effect on the Si–O bond, greatly weakening the Si–O bond strength and effectively reducing the viscosity of the glass melt and enhancing its fluidity [21]. In the present work, only the relative mass content of Na_2O and K_2O was changed, the amount of Na_2O was more than that of K_2O at the same mass percentage due to its low molecular weight. Therefore, with an increase in the amount of R^+ in the glaze, the glaze firing temperature and glaze melt viscosity gradually decreased, which would facilitate the large bubbles produced by the green body and glaze during the firing process to be discharged smoothly, eventually leaving the small bubbles to be uniformly distributed in the middle of the glaze layer. Moreover, the glaze

pinholes and other defects in the glaze surface could be effectively reduced. However, too high of an R^+ content would also lower the glaze melting temperature and the viscosity of the glaze melt. The bubbles originally located in the middle of the glaze layer gradually grow instead and are released to the glaze layer one after another, giving rise to a large number of pinholes in the glaze. Consequently, the glaze glossiness of the sample increased at first and then decreased with an increase in $\text{Na}_2\text{O}/\text{K}_2\text{O}$ (Figure 1).

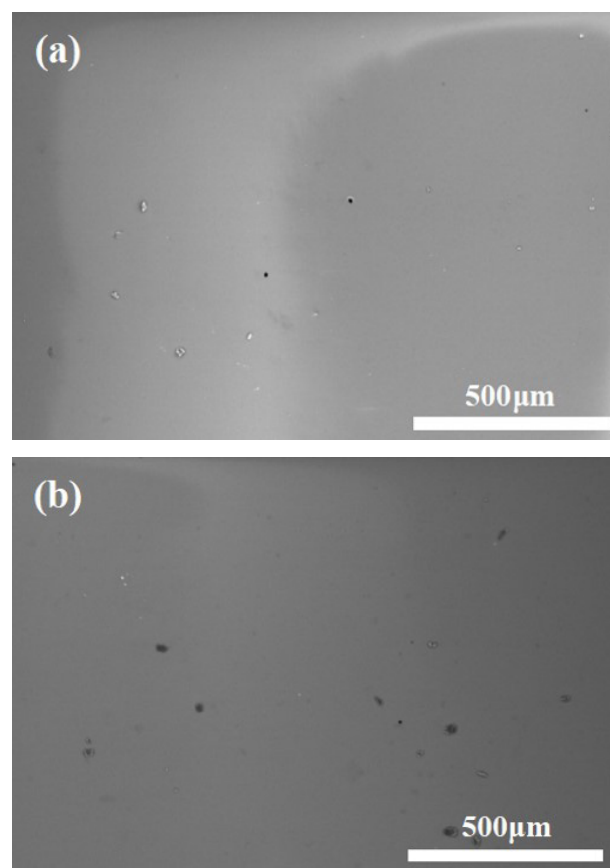


Figure 2. SEM images of the ceramic glaze surface. (a): sample A1 prepared at $\text{Na}_2\text{O}/\text{K}_2\text{O} = 1.2$, $\text{R}_2\text{O}/\text{Al}_2\text{O}_3 = 1$ (b): sample A2 prepared at $\text{Na}_2\text{O}/\text{K}_2\text{O} = 2$, $\text{R}_2\text{O}/\text{Al}_2\text{O}_3 = 1$.

Figure 2 shows the SEM images of the glaze surface of the sample prepared under $\text{R}_2\text{O}/\text{Al}_2\text{O}_3 = 1$ and $\text{Na}_2\text{O}/\text{K}_2\text{O} = 1.2$ and 2, respectively. The number of pores on the glaze surface for sample A1 obtained at $\text{Na}_2\text{O}/\text{K}_2\text{O} = 1.2$ was obviously smaller than that of A2 obtained at $\text{Na}_2\text{O}/\text{K}_2\text{O} = 2$, which further proved

that the low viscosity of the glaze caused by too high of an $\text{Na}_2\text{O}/\text{K}_2\text{O}$ ratio was one of main reasons that led to the appearance of glaze pinholes on the glaze surface and the glaze glossiness.

Figure 3 shows the changes in the glossiness (GU) of the samples obtained from different $\text{Na}_2\text{O}/\text{K}_2\text{O}$ and $\text{R}_2\text{O}/\text{Al}_2\text{O}_3$ ratios. On the whole, the glaze glossiness first decreased and then increased with an increase in the $\text{R}_2\text{O}/\text{Al}_2\text{O}_3$ ratio. When $\text{Na}_2\text{O}/\text{K}_2\text{O} = 0.8 - 1.8$, $\text{R}_2\text{O}/\text{Al}_2\text{O}_3 = 0.8 - 1.2$, the glossiness of the glaze changed between 88.3 to 108.3, which was larger than that of the basic sample (Table 1). Whereas, when $\text{Na}_2\text{O}/\text{K}_2\text{O} = 2$, $\text{R}_2\text{O}/\text{Al}_2\text{O}_3 = 1 - 1.2$, the glossiness of the glaze varied from 80.9 to 91.7, being slightly lower as a whole.

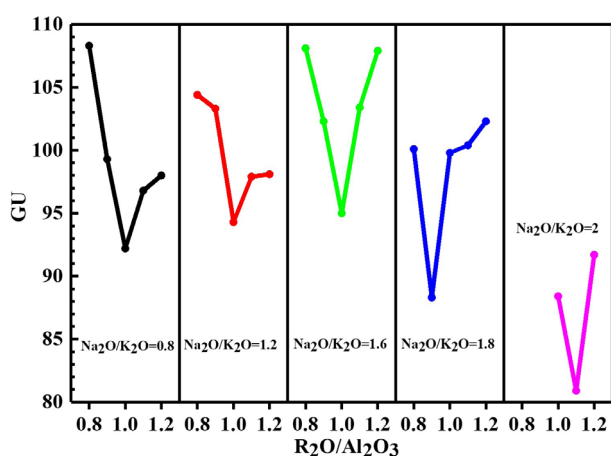


Figure 3. Variation trend in the ceramic glaze glossiness (GU) with $\text{R}_2\text{O}/\text{Al}_2\text{O}_3$.

The glossiness of the ceramic glaze has been found to also be affected by the reflectivity of the glaze. According to the calculation formula of the glaze reflectivity [20]: $R = (n - 1)^2 / (n + 1)^2$ (R is the reflectivity of the glaze and n is the refractive index of the glaze), the higher the refractive index, the higher the reflectivity, that is, the higher the glaze glossiness. With an increase in the alkali metal or alkaline earth metal oxide, the ratio of oxygen to silicon in the glass structure increases, and the three-dimensional network structure of the glass gradually disintegrates, which reduces the elastic modulus, chemical stability and viscosity of the glass. When the content of R_2O increases, the free oxygen content increases, which will destroy the network structure of the silicon-oxygen tetrahedron, resulting in a decrease in the glaze density, refractive index and glossiness. In addition, increasing the R_2O or decreasing the Al_2O_3 content in the glaze chemical composition is beneficial in reducing the firing temperature and high temperature viscosity of the glaze, which is not only conducive to the smooth elimination of air bubbles and improvement in the fluidity of the glaze melt, but it also closes the pits and reduces the pinholes on the glaze surface. Therefore, when

the $\text{Na}_2\text{O}/\text{K}_2\text{O}$ is constant, the glossiness increases with an increase in the $\text{R}_2\text{O}/\text{Al}_2\text{O}_3$ ratio (Figure 3).

On the other hand, it can be seen from Figure 3 that the glossiness showed the lowest value with the increase in the $\text{R}_2\text{O}/\text{Al}_2\text{O}_3$ ratio and the lowest value would decrease with the increase in the $\text{Na}_2\text{O}/\text{K}_2\text{O}$ ratio. The main reason may be speculated to be related to the increase in the amount of the alkali metal ions and free oxygen due to the molecular weight of Na_2O being less than that of K_2O . In general, the glass network structure is more likely to be further damaged with an increase in the free oxygen, resulting in a loose structure in the glaze layer and a decrease in the refractive index. Meanwhile, the decrease in the glaze glass firing temperature and viscosity may also give rise to the re-reaction between the substances in the glaze and green body to produce a large number of air bubbles, which will easily rush out of the glaze and result in a large number of pinholes in the glaze. Therefore, a decrease in the glaze density and the combined action of the glaze pinholes led to the low glossiness with an increase in the $\text{Na}_2\text{O}/\text{K}_2\text{O}$ ratio as a whole.

From Figure 1 and Figure 2, it can be seen that the glossiness obviously changed with the $\text{Na}_2\text{O}/\text{K}_2\text{O}$ and $\text{R}_2\text{O}/\text{Al}_2\text{O}_3$ ratios, which was mainly the result of the joint action of the glaze network structure and high temperature performance of the glaze. Therefore, in order to obtain a higher gloss glaze, it is necessary to adjust the chemical composition of the glaze to make the network compactness of the glaze and the high temperature properties of the glaze to be in a suitable range.

Glaze properties

Wettability and surface energy of the glaze

Figure 4 shows the changes in the surface energy, polarity ratio and water contact angle of the samples obtained under the different ratios of $\text{R}_2\text{O}/\text{Al}_2\text{O}_3$ and $\text{Na}_2\text{O}/\text{K}_2\text{O}$. The surface energy and polarity ratio of the glaze increased at first and then decreased with an increase in the $\text{Na}_2\text{O}/\text{K}_2\text{O}$ ratio. When $\text{Na}_2\text{O}/\text{K}_2\text{O} = 0.8 - 1.6$ and $\text{R}_2\text{O}/\text{Al}_2\text{O}_3 = 0.8 - 1.2$, the surface energy of glaze varied between 70.17 - 78.5 $\text{mJ}\cdot\text{m}^{-2}$, being greater than that of the basic glaze sample (Table 1). When $\text{Na}_2\text{O}/\text{K}_2\text{O}$ was more than 1.6, the surface energy of the sample began to obviously decrease. In addition, it can be seen from the above picture that the surface energy and the polarity ratio show a similar change in trend, while the contact angle of water showed an opposite trend to the surface energy.

Water molecules are a strong polar molecule, it is easy to form a strong affinity on the ceramic glaze with a large proportion of surface free energy polarity. The solid surface energy originates from the periodic and repetitive interruption of the solid surface atoms, which destroys the symmetry of the particle force field on the surface, resulting in the surface atom being

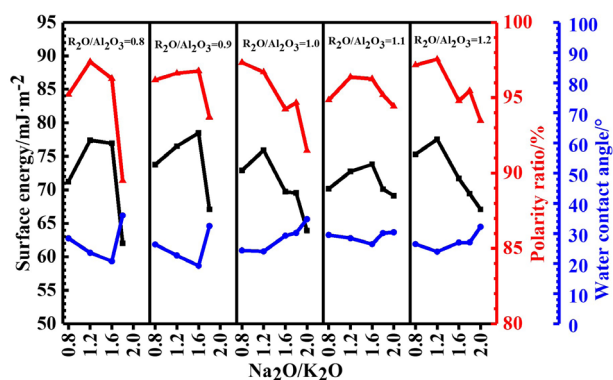


Figure 4. Variation trend in the ceramic glaze surface energy, polarity ratio and water contact angle with $\text{Na}_2\text{O}/\text{K}_2\text{O}$.

in a non-uniform force field, eventually showing an increasing energy and remaining a bonding force. For the silicate glass network structure, because the network forming ions have a relatively small radius and a high electric field strength, they can form an ion covalent bond with O^{2-} , providing a large bond force [22, 23]. Moreover, the greater the bond force inside the surface, the greater the surface energy and the density of the network structure. Thus, the amount of bridging oxygen atoms would directly affect the surface energy. Zhou [24] found that there were broken bonds ($\text{Si}-\text{O}^{2-}$) on the glaze surface, which could form hydroxyl groups with water through a chemical adsorption, and these hydroxyl groups continued to adsorb water molecules through physical adsorption. These two kinds of adsorption finally caused the glaze surface to have polarity and hydrophilicity. Thus, the amount of non-bridging oxygen atoms in the glaze would also affect the hydrophilicity of the glaze. Nevertheless, an increase in the number of broken bonds also negatively affects the hardness and corrosion resistance of the glaze. Therefore, in order to obtain ideal ceramic products, it is necessary to ensure that they have an improved glaze surface energy and an appropriate network density at the same time.

Alkali metal oxides are one of important influencing factors on the glaze glass network. Changes in the ratios of potassium to sodium oxides and their relative amount to Al_2O_3 ($\text{R}_2\text{O}/\text{Al}_2\text{O}_3$) are intimately related with the amount of non-bridging oxygen or bridging oxygen atoms in the glaze. Although increasing the proportion of Na_2O can enhance its destructive effect on the glass network structure in favour of obtaining a high gloss glaze, the increase of the $\text{Si}-\text{O}^{2-}$ amount in the glaze is conducive to the formation of hydrogen bonds between the glaze and water molecules to increase the surface polarity and surface energy. Therefore, as shown in Figure 4, the surface energy increased with an increase in the $\text{Na}_2\text{O}/\text{K}_2\text{O}$ ratio, but the loose network structure caused by the increase of the non-bridging oxygen atoms weakened the internal bond force of the glaze, leading to a decrease in the surface energy at a high $\text{Na}_2\text{O}/\text{K}_2\text{O}$ ratio.

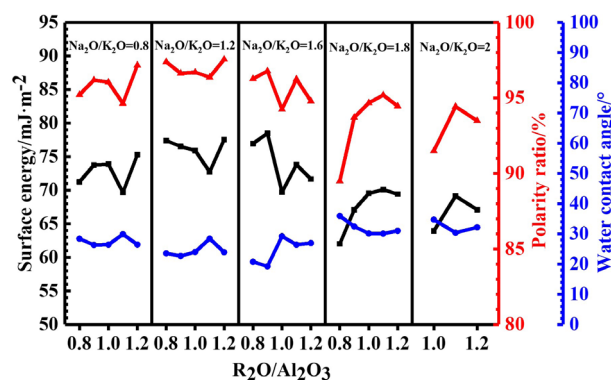


Figure 5. Variation trend in the ceramic glaze surface energy, polarity ratio and water contact angle with $\text{R}_2\text{O}/\text{Al}_2\text{O}_3$.

Figure 5 shows the changes in the surface energy, polarity ratio and water contact angle with the different $\text{Na}_2\text{O}/\text{K}_2\text{O}$ and $\text{R}_2\text{O}/\text{Al}_2\text{O}_3$ ratios. When $\text{Na}_2\text{O}/\text{K}_2\text{O}$ varied between 0.8 to 1.6, the surface energy first decreased and then increased with the $\text{R}_2\text{O}/\text{Al}_2\text{O}_3$ ratio, giving a surface energy of $70.17 - 78.5 \text{ mJ}\cdot\text{m}^{-2}$, which was larger than that of the basic sample (Table 1). Under $\text{Na}_2\text{O}/\text{K}_2\text{O} = 1.8 - 2$, the surface energy gradually increased with the $\text{R}_2\text{O}/\text{Al}_2\text{O}_3$ ratio before $\text{R}_2\text{O}/\text{Al}_2\text{O}_3 = 2$, giving a surface energy of $62.02 - 70.03 \text{ mJ}\cdot\text{m}^{-2}$, being smaller than that of the basic sample. As discussed in the previous section, the $\text{R}_2\text{O}/\text{Al}_2\text{O}_3$ ratio is directly related to the role of Al_2O_3 in the glass network structure. Because the $\text{R}_2\text{O}/\text{Al}_2\text{O}_3$ (mol. %) designed here was more than 1, Al^{3+} existed in a tetrahedron as a network-forming body [25]. However, when the efficiency of increasing the number of interruption bonds in the glass network on increasing the surface energy is less than that of weakening the internal bond force on the glaze, the surface energy will decrease as a whole. Therefore, when $\text{Na}_2\text{O}/\text{K}_2\text{O} = 0.8 - 1.6$ and $\text{R}_2\text{O}/\text{Al}_2\text{O}_3 = 0.8 - 1.1$, or when $\text{Na}_2\text{O}/\text{K}_2\text{O} = 1.8 - 2$ and $\text{R}_2\text{O}/\text{Al}_2\text{O}_3 = 1.1 - 1.2$, the surface energy decreased with an increase in the $\text{R}_2\text{O}/\text{Al}_2\text{O}_3$ ratio. Conversely, when the efficiency of the increase in the surface energy has greater than that of the weakening of the internal bond force on the glaze, the surface energy will increase as a whole. Therefore, when $\text{Na}_2\text{O}/\text{K}_2\text{O} = 0.8 - 1.6$ and $\text{R}_2\text{O}/\text{Al}_2\text{O}_3 = 1.1 - 1.2$, or when $\text{Na}_2\text{O}/\text{K}_2\text{O} = 1.8$ and $\text{R}_2\text{O}/\text{Al}_2\text{O}_3 = 0.8 - 1.1$, the surface energy increased with an increase in the $\text{R}_2\text{O}/\text{Al}_2\text{O}_3$ ratio. In addition, it can be seen from Figure 5 that the overall surface energy of the samples obtained at $\text{Na}_2\text{O}/\text{K}_2\text{O} = 1.8 - 2$ was lower than that at $\text{Na}_2\text{O}/\text{K}_2\text{O} = 0.8 - 1.6$, which was speculated to be mainly attributed to the great damage caused by the high amount of R_2O .

Increasing the network compactness of the glaze layer and increasing the number of broken bonds on the glaze surface will increase the surface energy of the glaze, but the denser the network structure of the glaze layer reduces the number of broken bonds on the glaze surface. Thus, adjusting the chemical

composition of the glaze, especially the $\text{Na}_2\text{O}/\text{K}_2\text{O}$ and $\text{R}_2\text{O}/\text{Al}_2\text{O}_3$ ratio to make the network density and network compactness of the glaze layer to be within a suitable range could provide a useful route to prepare a ceramic glaze with high surface energy and high gloss, and to facilitate an improvement in the stain resistance and easy cleaning performance of the ceramic glaze.

Structural analysis

Figure 6 shows the ^{29}Si MAS-NMR spectra of samples A1 and A2 prepared at $\text{R}_2\text{O}/\text{Al}_2\text{O}_3 = 1$, $\text{Na}_2\text{O}/\text{K}_2\text{O} = 1.2$ and 2, respectively. Both samples A1 and A2 have a wide ^{29}Si MAS-NMR band in the $-120 \sim -60$ ppm range, and the absolute value for the A1 chemical shift was greater than that for A2. Ananthanarayanan [26] pointed out that the wide resonance spectrum of silicate glass could be decomposed into three independent resonances with a different Q_n (where n is the number of bridging oxygen bound to Si, that is, Q_4 is $[\text{SiO}_4]$, Q_3 is $[\text{SiO}_3\text{O}^{2-}]$, Q_2 is $[\text{SiO}_2\text{O}_2^{2-}]$). Chen's ^{29}Si MAS-NMR spectra study on borosilicate glass indicated that the peak located at $-70 \sim -90$ ppm, $-90 \sim -106$ ppm and $-100 \sim -120$ ppm belonged to Q_2 , Q_3 and Q_4 , respectively [27]. According to the literature, the three resonance spectra at -83 , -91 and -100 ppm in this experiment should be attributed to Q_2 , Q_3 and Q_4 , respectively. It can be seen from the peak separation results that the Q_3 peak area ratio of samples A1 and A2 was much larger than that of Q_4 and Q_2 , and the Q_2 area values of the two samples were similar. Although the area proportion of Q_4 for sample A1 was larger than that for A2, the proportion of Q_3 was less than A2. Such a result should be related the amount of non-bridging oxygen in the glaze glass network. Since sample A2 contained a high $\text{Na}_2\text{O}/\text{K}_2\text{O}$ ratio, much more alkali metal ions would exert a destructive effect on the network structure of glaze glass and increase the amount of non-bridging oxygen, resulting in a relatively loose glass network structure, so that the Q_3 of A2 was larger than A1, and the surface energy of A1 was also larger.

In addition, according to the calculation formula of the bridging oxygen number of aluminosilicate glass, when $(\text{R}_2\text{O} + \text{RO})/\text{Al}_2\text{O}_3$ (mol. %) > 1 , $X = \text{O}/(\text{Si} + \text{Al})$ (mol. %), the bridging oxygen number Y can be expressed as $Y = 8 - 2X$ [28], the theoretical bridging oxygen number Y of samples A1 and A2 was 3.425 and 3.413, respectively, that is, the network structure of A1 was slightly denser than A2 in theory.

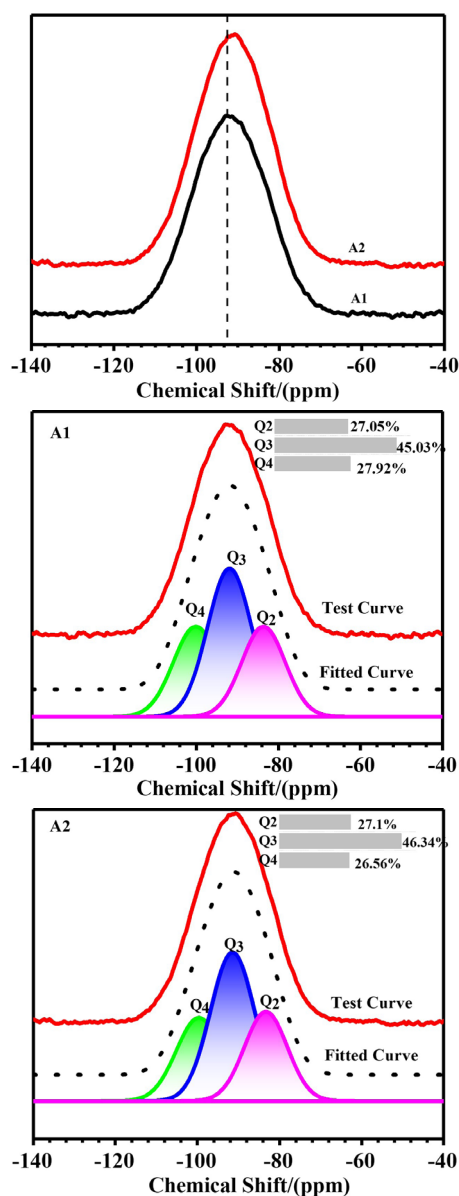


Figure 6. The ^{29}Si MAS-NMR spectra and their peaks of samples A1 and A2 (the correlation coefficient of the fitting R^2 for each sample is more than 0.99).

Furthermore, it can be seen from Figure 6 that the absolute value of the peak position of A1 was greater than that of A2 [29] and the proportion of Q_4 was also slightly higher than that of A2. The above detected results also further confirmed that the polymerisation degree of A1 was indeed greater than that of A2, leading to a denser structure and showing a higher surface energy of $11.98 \text{ mJ}\cdot\text{m}^{-2}$ than that of A2.

Table 2. Chemical composition and glaze properties of A1 and A2.

Samples	Chemical composition (wt. %)								Glaze properties			
	SiO_2	Al_2O_3	CaO	MgO	Na_2O	K_2O	$\text{Na}_2\text{O}/\text{K}_2\text{O}$	$\text{R}_2\text{O}/\text{Al}_2\text{O}_3$	γ_s ($\text{mJ}\cdot\text{m}^{-2}$)	γ_s^d (%)	Gloss	Y
A1	60.56	11.42	14.54	2.07	6.23	5.19	1.2	1	75.91	96.7	94.3	3.425
A2	60.56	11.42	14.54	2.07	7.61	3.81	2	1	63.93	91.5	88.4	3.413

CONCLUSIONS

The glossiness and surface energy of the ceramic glaze could be effectively improved by adjusting the R_2O/Al_2O_3 and Na_2O/K_2O ratios in the chemical composition on the basis of the basic glaze. The ceramic glaze obtained had small numbers of pinholes and showed a high surface energy and good water wettability and glossiness. Its surface energy was mainly affected by the internal network structure. The compactness of the network structure in the glaze layer together with the broken bond determined the surface energy and water wettability. The greater the surface energy of the glaze was, the greater the polarity component was, and the better the wettability of water on the glaze was, which would be conducive to improving the anti-fouling and easy cleaning of ceramic products. The improvement in the glaze glossiness was mainly due to the high network density of the glaze layer and the suitable high temperature viscosity and firing temperature, and the improvement of glaze surface energy was mainly due to the increase in the density of glaze network and the increase in the number of broken bonds on the glaze. When $Na_2O/K_2O = 0.8 - 1.6$, $R_2O/Al_2O_3 = 0.8 - 1.2$, the surface energy was $70.17 - 78.5 \text{ mJ}\cdot\text{m}^{-2}$ and the gloss was $88.3 - 108.3$, being obvious higher than those of the basic glaze.

Acknowledgments

This work was supported by the National Key Research and Development Plan of China (Grant No. 2022YFE0197200).

REFERENCES

- Jing J Q. (2008): Development of anti-fouling ceramic glaze. *Chinese Ceramics*, 44, 3. Doi: 10.3969/j.issn.1001-9642.2008.11.016
- Zhang D G, Li L H. (2018): One-step method for fabrication of superhydrophobic and superoleophilic surface for water-oil separation. *Colloids and Surfaces*, 552, 32-38. Doi: 10.1016/j.colsurfa.2018.05.006
- Gong A, Zheng Y. (2021): Spray fabrication of superhydrophobic coating on aluminum alloy for corrosion mitigation. *Materials Today Communications*, 26, 101828. Doi: 10.1016/j.mtcomm.2020.101828
- Zhu R F, Liu M M. (2020): One-pot preparation of fluorine-free magnetic superhydrophobic particles for controllable liquid marbles and robust multifunctional coatings. *ACS Applied Materials and Interfaces*, 12, 17004-17017. Doi: 10.1021/acsmi.9b22268
- Yang C, Cui S H. (2021): Scalable superhydrophobic T-shape micro/nano structured inorganic alumina coatings. *Chemical Engineering Journal*, 409, 128142. Doi: 10.1016/j.ccej.2020.128142
- Tang Y, Yang X L. (2021): Robust micro-nanostructured superhydrophobic surfaces for long-term dropwise condensation. *Nano Letters*, 21, 9824-9833. Doi: 10.1021/acs.nanolett.1c01584
- Huang W X, Lei M. (2010): Effect of polyethylene glycol on hydrophilic TiO_2 films: porosity-driven superhydrophilicity. *Surface and Coatings Technology*, 204, 3954-3961. Doi: 10.1016/j.surfcoat.2010.03.030
- Mao C C, Wang X. (2021): Super-hydrophilic TiO_2 -based coating of anion exchange membranes with improved antifouling performance Colloid. *Colloids and Surfaces A-physicochemical and Engineering Aspects*, 614, 126-136. Doi: 10.1016/j.colsurfa.2021.126136
- Li N, Kuang J. (2021): Fabrication of transparent superhydrophilic coatings with self-cleaning and anti-fogging properties by using dendritic nano-silica. *Ceramics International*, 47, 18743-18750. Doi: 10.1016/j.ceramint.2021.03.209
- Ishiguro H, Nakano R. (2011): Photocatalytic inactivation of bacteriophages by TiO_2 -coated glass plates under low-intensity, long-wavelength UV irradiation. *Photochemical and Photobiological Sciences*, 10, 1825-1829. Doi: 10.1039/c1pp05192j
- Adam C. M., Nathan P. M. (2021): Ag-doped Bioactive Glass-Ceramic 3D Scaffolds: Microstructural, Antibacterial, and Biological Properties. *Journal of the European Ceramic Society*, 41, 3717-3730. Doi: 10.1016/j.jeurceramsoc.2021.01.011
- Moghaddasi Z, Mohammadzadeh M R. (2022): Synthesis and effectiveness of Cu-infused TiO_2 - SiO_2 based self-cleaning and antibacterial thin-films coating on ceramic tiles. *Sol-Gel Science and Technology*, 103, 396-404. Doi: 10.1007/s10971-022-05853-6
- Kim J, Jeong D, Choi J. (2022): Changes in the glaze characteristics and moderate antibacterial activity of ceramic tile glazes with the addition of ZnO. *Asian Ceramic Societies*, 10, 241-252. Doi: 10.1080/21870764.2022.2038044
- Makoto H, Koichi H, Masami A. (2003): Sanitary earthen products. EP1149810 A1
- Si Y F, Dong Z C, Jiang L. (2018): Bioinspired designs of superhydrophobic and superhydrophilic materials. *ACS Central Science*, 4, 1102-1112. Doi: 10.1021/acscentsci.8b00504
- Gao Y H, Hao W R. (2022): Enhancement of superhydrophilic/underwater super-oleophobic performance of ceramic membrane with TiO_2 nanowire array prepared via low temperature oxidation. *Ceramics International*, 48, 9426-9433. Doi: 10.1016/j.ceramint.2021.12.139
- Yuan L, Wen T P. (2021): Modified superhydrophilic/underwater superoleophobic mullite fiber-based porous ceramic for oil-water separation. *Materials Research Bulletin*, 143, 111454. Doi: 10.1016/j.materresbull.2021.111454
- Fan Z R, Zhou S Y. (2021): A novel ceramic microfiltration membrane fabricated by anthurium andraeanum-like attapulgite nanofibers for high-efficiency oil-in-water emulsions separation. *Journal of Membrane Science*, 630, 119291. Doi: 10.1016/j.memsci.2021.119291
- Azimi M, Asselin E. (2021): Chemical oxidation of high-density polyethylene: Surface energy, functionality, and adhesion to liquid epoxy. *Journal of Applied Polymer Science*, 138, 1-14. Doi: 10.1002/app.50999
- Wang A H. (2001): On the glossiness of daily ceramic glaze. *Ceramic Research*, 16, 30-33. Doi: 10.3969/j.issn.1000-9892.2001.04.009

21. Zhou X Y. (2015): Effect of alkali metal oxides on viscosity and crystallization properties of CaO-MgO-Al₂O₃-SiO₂ glass. *Journal of Wuhan University of Technology*, 37, 42-47. Doi: 10.3963/j.issn.1671-4431.2015.03.002
22. Hu S H. (2008): Effect of surface free energy on the cleanability of ceramic glaze. *Journal of Silicate*, 36, 1282-1287. Doi: 10.3321/j.issn:0454-5648.2008.09.018
23. Zhao Y X, Liu Y. (2014): Molecular dynamics simulation on diffusion behaviors of alkali metal Ions in electronic glasses. *Journal of Yanshan University*, 41, 304-310. Doi: 10.3969/j.issn.1007-791X.2017.04.004
24. Zhou J. (2013): Influence of composition on microscopy defects on the zirconium fritted glaze surface. *Ceramics China*, 51, 76-87.
25. Yu Y T, Wang B, Wang M Y. (2017): Reactive Molecular Dynamics Simulations of Sodium Silicate Glasses: Toward an Improved Understanding of the Structure. *International Journal of Applied Glass Science*, 8, 276-284. Doi: 10.1111/ijag.12248
26. Ananthanarayanan A, Kothiyal G P, Montagne L. (2010): MAS-NMR investigations of the crystallization behaviour of lithium aluminum silicate (LAS) glasses containing P₂O₅ and TiO₂ nucleants. *Journal of Solids State Chemistry*, 183, 1416-1422. Doi: 10.1016/j.jssc.2010.04.011
27. Chen Y J, Zhu S Z. (2021): Study on the structure change and devitrification of high silica glass particles with B₂O₃ modification by Raman, IR and MAS NMR spectroscopies. *Journal of Non-Crystalline Solids*, 573, 1-7. Doi: 10.1016/j.jnoncrysol.2021.121144
28. Lin Z S. (2013): Inorganic nonmetallic materials technology. 4th ed. *Wuhan University of Technology Press*
29. Zhou Z Q, He F. (2022): Influences of Al₂O₃ content on crystallization and physical properties of LAS glass-ceramics prepared from spodumene. *Journal of Non-Crystalline Solids*, 576, 1-9. Doi: 10.1016/j.jnoncrysol.2021.121256